Arabian Journal of Chemistry (2014) xxx, xxx–xxx

King Saud University

Arabian Journal of Chemistry

www.ksu.edu.sa
www.sciencedirect.com

ORIGINAL ARTICLE

Reduction of graphene oxide nanosheets by natural beta carotene and its potential use as supercapacitor electrode

Rubaiyi M. Zaid [a], Fui Chin Chong [a], Ellie Yi Lih Teo [c], Eng-Poh Ng [b], Kwok Feng Chong [c,*]

[a] *Faculty of Chemical and Natural Resources Engineering, Universiti Malaysia Pahang, 26300 Gambang, Kuantan, Malaysia*
[b] *School of Chemical Sciences, Universiti Sains Malaysia, 11800 Penang, Malaysia*
[c] *Faculty of Industrial Sciences & Technology, Universiti Malaysia Pahang, 26300 Gambang, Kuantan, Malaysia*

Received 26 February 2014; accepted 25 November 2014

KEYWORDS

Beta carotene;
Deoxygenation;
Reduced graphene oxide;
Supercapacitor

Abstract A green, non-toxic and eco-friendly approach for the reduction of graphene oxide (GO) nanosheets using natural β-carotene is reported. The FTIR spectroscopy and thermogravimetric analyses reveal the oxygen scavenging property of β-carotene successfully removes oxygen functionalities on GO nanosheets. Complete GO reduction is achieved within 16 h with 10 mM β-carotene as confirmed by the UV spectroscopy results. The high resolution transmission electron microscopy images provide clear evidence for the formation of few layers of graphene nanosheets. Furthermore, the mechanism of GO reduction by β-carotene has been proposed in this study. The electrochemical testing shows good charge storage properties of β-carotene reduced GO (142 F/g at 10 mV/s; 149 F/g at 1 A/g in Na_2SO_4), with stable cycling (89%) for up to 1000 cycles. The findings suggest the reduction of GO nanosheets by β-carotene is a suitable approach in producing graphene nanosheets for supercapacitor electrode.

1. Introduction

The green development of novel materials with superior properties is a main concern faced by modern chemistry. In this context, the advances in nanotechnology have led to the synthesis of novel materials in order to meet the increasing demand of the industries for advanced functional materials. Graphene, a two-dimensional array of sp^2-hybridized carbon atoms in honeycomb lattice, represents a conceptually new class of materials since its first discovery in 2004 (Novoselov et al., 2004). Unlike other nanomaterials,

* Corresponding author. Tel.: +60 9 5492403.
E-mail address: ckfeng@ump.edu.my (K.F. Chong).
Peer review under responsibility of King Saud University.

Production and hosting by Elsevier

http://dx.doi.org/10.1016/j.arabjc.2014.11.036
1878-5352 © 2014 The Authors. Production and hosting by Elsevier B.V. on behalf of King Saud University.
This is an open access article under the CC BY-NC-ND license (http://creativecommons.org/licenses/by-nc-nd/3.0/).

Please cite this article in press as: Zaid, R.M. et al., Reduction of graphene oxide nanosheets by natural beta carotene and its potential use as supercapacitor electrode. Arabian Journal of Chemistry (2014), http://dx.doi.org/10.1016/j.arabjc.2014.11.036

graphene nanosheets exhibit exceptionally high mechanical, thermal and electronic qualities (Novoselov et al., 2005; Lee et al., 2008; Balandin, 2011). These unique properties thus make graphene a promising material for a wide variety of new technological applications such as solar cells (Wang et al., 2009), fuel cells (Jeon et al., 2013; Ng et al., 2010), batteries (Mukhopadhyay et al., 2013), ultracapacitors (Stoller et al., 2008), fiber polarizers (Bao et al., 2011) and gas sensors (Schedin et al., 2007).

Several approaches for fabricating graphene nanosheets such as chemical vapor deposition (CVD) (Petrone et al., 2012; Ismach et al., 2010), epitaxial growth (Strupinski et al., 2011) and chemical reduction of exfoliated graphite oxide (Stankovich et al., 2007) have been reported where the latter one is preferable, due to its cost effectiveness and bulk-scale production feasibility (Park and Ruoff, 2009). Typically, the synthesis of chemically reduced graphene is achieved by oxidation of graphite, followed by exfoliation to produce graphene oxide (GO), and finally GO reduction using hydrazine as a reducing agent. The conventional condition, however, formulates the synthesis of chemically reduced graphene as not eco-friendly due to the consumption of extremely toxic and potentially explosive hydrazine as reducing agent (Li et al., 2008). Thus, any new insight to replace the hazardous chemicals in the synthesis of graphene nanosheets is urgently needed.

The reduction of GO using more eco-friendly and non-toxic reducing agents such as ascorbic acid (vitamin C) was first reported by Fernández-Merino and co-workers (2010). They reported that the ascorbic acid has similar deoxygenation efficacy as hydrazine in the reduction of GO and the reduction can be performed either in organic or aqueous solvents. Since then, non-toxic compounds such as starch-based materials (Feng et al., 2013), rose water (Haghighi and Tabrizi, 2013), tea polyphenol (Wang et al., 2011), aqueous phytoextracts (Thakur and Karak, 2012), sugar (Zhu et al., 2010) and yeast (Khanra et al., 2012) have been reported as potential replacement for hydrazine as reducing agents in graphene synthesis.

β-Carotene is a natural product that could abundantly be found in fruits and vegetables. It is composed of polyunsaturated hydrocarbons with two retinyl groups and it has been proven as a powerful anti-oxidant with excellent singlet oxygen scavenging property that prevents attack of free radicals in the body (Ciccone et al., 2013). Its abundance in food and non-toxic nature could be the interest in mass production of chemically reduced graphene, which could potentially reduce the production cost as well as the toxic waste. Thus, its deoxygenation efficacy in the synthesis of chemically reduced graphene is worth to be further explored.

Herein, we report the reduction of GO using β-carotene and the process is monitored by spectroscopic and microscopic techniques. The deoxygenation performance of β-carotene is then compared with the hydrazine reducing system. Furthermore, an investigation into the charge storage properties of β-carotene reduced GO using electrochemical analysis is also explored for the potential use as a supercapacitor electrode.

2. Experimental section

2.1. Preparation of graphene oxide (GO), β-carotene reduced graphene oxide (CRGO) and hydrazine reduced graphene oxide (HRGO)

Prior to GO preparation, graphite powder (50 μm, ⩾99.5%, Merck) was pre-oxidized in order to prevent incomplete oxidation. Briefly, graphite powder (20.00 g) was added into a solution containing H_2SO_4 (30 mL, 95%, Sigma–Aldrich), $K_2S_2O_8$ (10.00 g, ⩾99.0%, Sigma–Aldrich) and P_2O_5 (10.00 g, 99.99%, Sigma–Aldrich) prior to heating at 80 °C for 6 h. The mixture was then diluted with distilled water, filtered and washed until the filtrate became neutral in pH. The pre-oxidized graphite powder was dried overnight at room temperature before being subjected to oxidation using Hummers' method (Hummers and Offeman, 1958). The pre-oxidized graphite powder (20.00 g) was added into H_2SO_4 solution (460 mL), followed by the addition of $KMnO_4$ powder (60.00 g, 99%, Merck). The addition of $KMnO_4$ powder was done slowly with stirring and cooling to maintain the temperature of the mixture at 20 °C. The mixture was then stirred at 35 °C for 2 h before the addition of distilled water (1 L). The stirring was continued for 15 min and additional distilled water (3 L) and H_2O_2 (50 mL, 30 wt.%, Sigma–Aldrich) were then added into the mixture. The mixture was filtered, washed with 1:10 HCl (37%, Fluka) and dried overnight (60 °C) in vacuum to obtain the dry graphite oxide. The exfoliation of graphite oxide was done by sonicating (200 W) the graphite oxide dispersion (2 mg/mL) for 30 min. The unexfoliated graphite oxide was then removed by centrifugation (10,000*g*) for 10 min. The remaining homogeneous yellow brown supernatant was obtained as GO dispersion.

The CRGO was prepared by adding appropriate amounts of β-carotene (97%, Sigma) into GO dispersion (50 mL) and the mixture was refluxed at 95 °C for 24 h. The dried CRGO was obtained by vacuum filtration, washing with distilled water and drying overnight (60 °C) in vacuum. A similar procedure was also applied to HRGO except hydrazine monohydrate (0.25 mL, 98%, Sigma–Aldrich) was used to replace β-carotene as reductant.

2.2. Characterization

The degree of GO reduction was monitored using a Thermo Scientific (Genesys 10S) UV spectrophotometer. The functional groups of samples were confirmed by using a Perkin Elmer (Spectrum 100) infrared spectrophotometer over the range of 400–4000 cm^{-1}. The thermal stability was determined with a TA Instrument (Q500) thermal analyzer heating from room temperature to 700 °C at a heating rate of 10 °C/min in N_2 environment. The crystal structures of samples were analyzed using a Rigaku X-ray diffractometer (Miniflex II with Cu-K_α radiation at 40 kV, 30 mA, λ = 1.5406 Å) within the 2θ range of 5° to 90° at a scanning rate of 1° per second with a step time of 2 s. The surface morphology and nanosheet thickness were studied by PHILIPS (CM-12) transmission electron microscope (TEM) with an accelerating voltage of

Please cite this article in press as: Zaid, R.M. et al., Reduction of graphene oxide nanosheets by natural beta carotene and its potential use as supercapacitor electrode. Arabian Journal of Chemistry (2014), http://dx.doi.org/10.1016/j.arabjc.2014.11.036

Table 1 Reduction of GO by β-carotene as a function of concentration and time.

Functions	Reductant concentration (mM)	Reaction time (h)	Absorption peak position (nm)
Reductant concentration	1	24	244
	2	24	251
	5	24	264
	10	24	270
	12	24	270
Reduction time	10	0	230
	10	2	237
	10	3	242
	10	7	263
	10	16	270
	10	24	270

200 kV. The defects in graphene were examined by using a Renishaw (In-via) Raman microscope with 532 nm laser as the excitation source.

2.3. Electrochemical study

Prior to electrochemical measurement, a glassy carbon electrode (CH Instruments) was polished with alumina powders and was sequentially sonicated in deionized water and anhydrous ethanol. The CRGO electrode was made by drop casting CRGO suspension (in *N*-2-methyl-pyrrolidone (99%, Aldrich)) onto the polished glassy carbon electrode. A three-electrode system was constructed for electrochemical study with CRGO electrode as a working electrode, platinum wire (CH Instruments) as a counter electrode, and Ag/AgCl (CH Instruments) as a reference electrode. Autolab (PGSTAT101) potentiostat/galvanostat was used to perform electrochemical study. Cyclic voltammetry (CV) tests were performed in the potential range between 0 V and 1 V versus Ag/AgCl with a scan rate from 10 to 100 mV/s. Charge–discharge galvanostatic tests were performed at a current density from 1 to 10 A/g.

Table 2 Comparison table for reducing efficacy of different natural reducing agents.

Reducing agent	Duration for complete reduction (h)	References
Ascorbic acid	24	Gao et al. (2010)
Ascorbic acid	24	Pruna et al. (2013)
L-ascorbic acid	48	Zhang et al., 2010
Dopamine	24	Xu et al. (2010)
Wild carrot root	24	Kuila et al. (2012)
β-Carotene	16	This work

3. Results and discussion

3.1. Optimization study

UV–Vis spectroscopy allows visualization of the formation of reduced GO since the reaction involves the restoration of C=C bonds. Time-dependence and concentration-dependence experiments were carried out and monitored with UV–Vis spectrophotometer to determine the optimal synthesis condition for CRGO. The shifting of UV absorption peak position as a function of concentration and time during the course of reduction is shown in Table 1. As shown in Fig. 1a, the initial position of absorption peak is at 230 nm where a shifting of absorption peak to 270 nm (due to restoration of electronic conjugation during reduction process) is identified as a complete reduction process (Fig. 1b) (Fernández-Merino et al., 2010). The reductant-concentration dependence kinetic study shows that the rate of reduction increases with the concentration of β-carotene where 10 mM of β-carotene is sufficient to complete the reduction of GO within 24 h (Table 1).

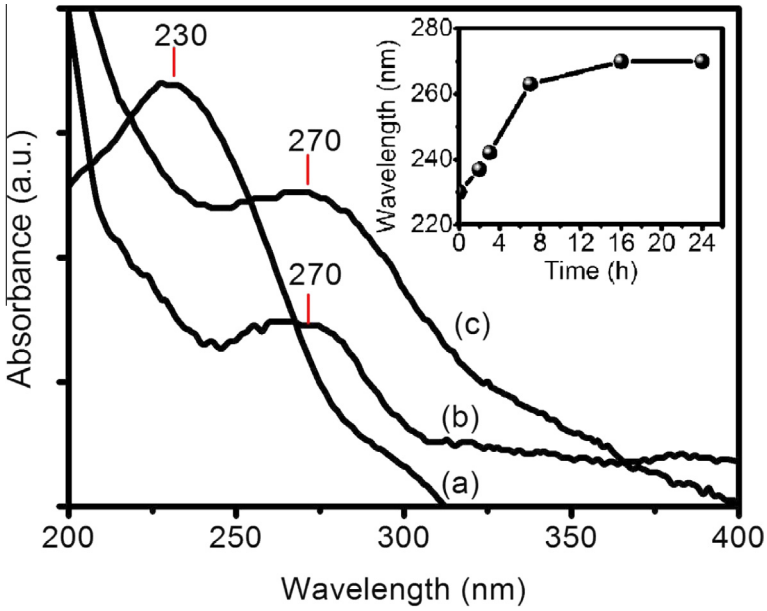

Figure 1 UV spectra of (a) GO, (b) CRGO and (c) HRGO. The reduction was performed using 10 mM reductants. Inset: UV–Vis absorption peak shifting of CRGO as a function of time.

Please cite this article in press as: Zaid, R.M. et al., Reduction of graphene oxide nanosheets by natural beta carotene and its potential use as supercapacitor electrode. Arabian Journal of Chemistry (2014), http://dx.doi.org/10.1016/j.arabjc.2014.11.036

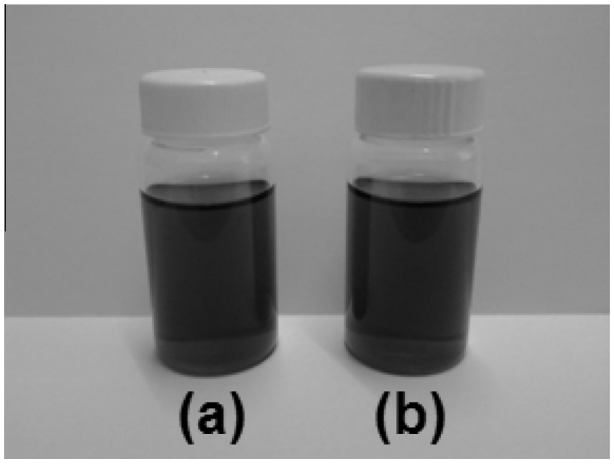

Figure 2 Visual observation of (a) CRGO and (b) HRGO suspensions in *N*-2-methyl-pyrrolidone after 2 weeks.

The reduction was also performed as a function of time while keeping the concentration of β-carotene constant (10 mM) to obtain the optimum reaction time. As shown in the inset of Fig. 1 and Table 1, at least 16 h of treatment is required to complete the GO reduction by β-carotene. For comparison, GO reduction by hydrazine was also conducted and the shifting of absorption peak to 270 nm could be observed, as shown in Fig. 1c. It can be clearly seen that in the reduction of GO, β-carotene is able to restore the electronic conjugation of reduced GO as hydrazine does. In addition, the reducing efficacy of β-carotene is also compared with other reported natural reducing agents and the performance is summarized as in Table 2. It can be seen that the β-carotene could complete GO reduction at a faster rate than ascorbic acid, dopamine or wild carrot root extracts.

The GO suspension has yellow brownish color in deionized water. After reduction by β-carotene, the reduced GO precipitated out as black sediment. Thus, this confirms with the UV–Vis spectroscopy data that the reduction of GO by β-carotene has successfully occurred. The CRGO colloidstable suspension in common organic solvent is vital in material manipulation and processing for practical applications. Thus, the CRGO suspension stability was tested on *N*-2-methyl-pyrrolidone solvent and it can be clearly observed that CRGO is colloidally stable in *N*-2-methyl-pyrrolidone solvent, showing no signs of precipitation even after 2 weeks

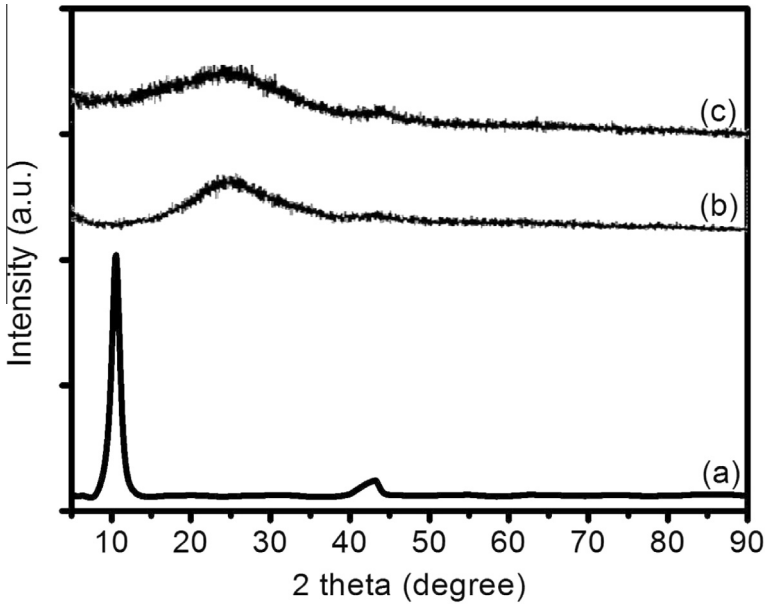

Figure 3 XRD diffraction patterns of (a) GO, (b) CRGO and (c) HRGO.

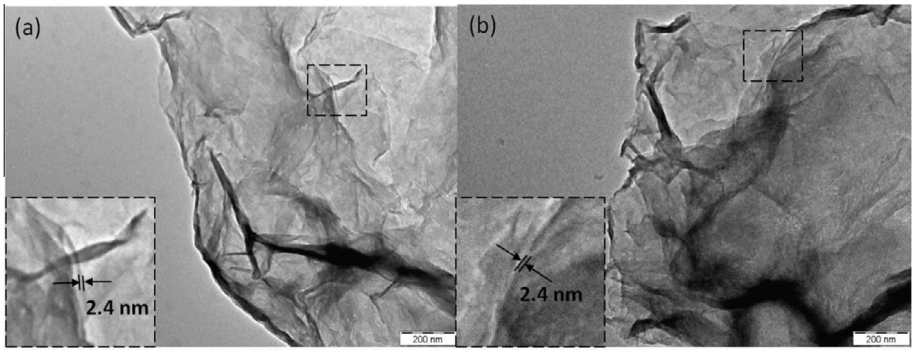

Figure 4 TEM images of (a) CRGO and (b) HRGO. Inset shows the sheet thickness at high magnification.

Please cite this article in press as: Zaid, R.M. et al., Reduction of graphene oxide nanosheets by natural beta carotene and its potential use as supercapacitor electrode. Arabian Journal of Chemistry (2014), http://dx.doi.org/10.1016/j.arabjc.2014.11.036

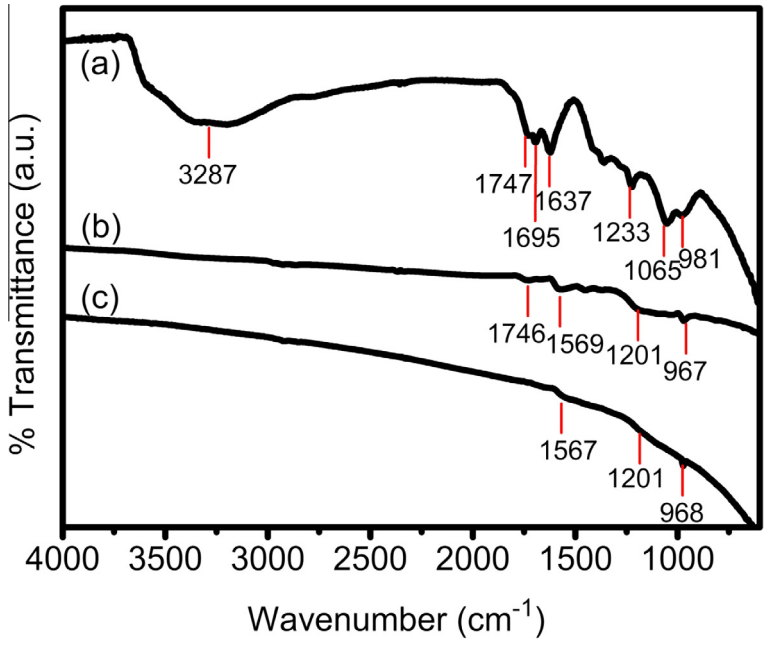

Figure 5 ATR-FTIR spectra of (a) GO, (b) CRGO and (c) HRGO.

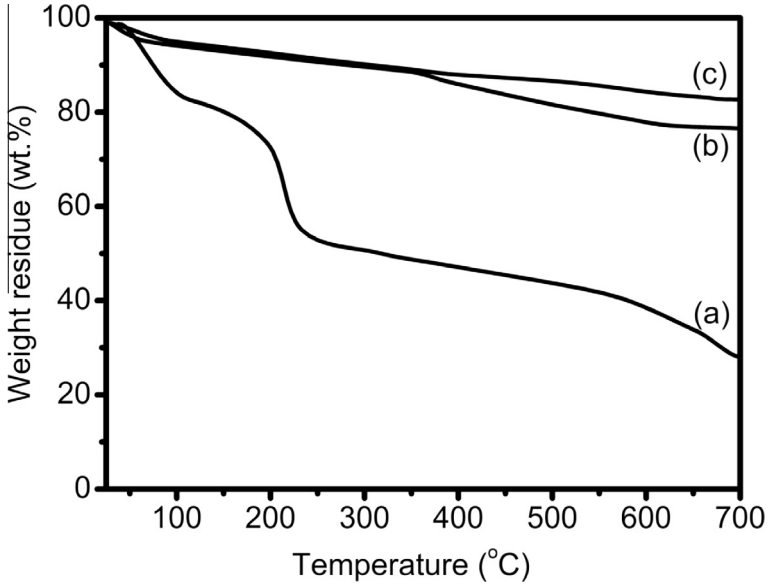

Figure 6 TGA plots of (a) GO, (b) CRGO and (c) HRGO.

(Fig. 2a). The CRGO suspension is also compared with that of HRGO (Fig. 2b) and there is no significant difference between both reduced samples in terms of color and colloid stability.

3.2. Structural analysis

The crystal nature of CRGO was confirmed by XRD analysis. Fig. 3 shows the XRD patterns of GO and CRGO where the diffractogram of HRGO is also included for comparison purposes. Initially, GO exhibits an intense diffraction peak (002) at 10.3°, which is corresponding to the *d*-spacing of 0.862 nm (Fig. 3a) (Moon et al., 2010). Upon GO reduction by β-carotene, the intensity of (002) diffraction peak decreases and the peak width is broadened due to the stacking of graphene layers. Furthermore, the signal is also shifted to 23.13° with a *d*-spacing of 0.392 nm (Fig. 3b). The decrease in *d*-spacing is attributed to the removal of oxygen functional groups and water molecules within GO sheets (Kuila et al., 2012). Furthermore, the XRD pattern of HRGO is also shown in Fig. 3c and similar diffraction patterns with broad diffraction band at similar 2θ position as CRGO are observed.

The morphology of CRGO was studied and compared with that of HRGO based on TEM analysis. Fig. 4 shows the TEM images of CRGO and HRGO. As shown, both reduced nanomaterials exhibit similar morphology with curvy and wrinkled sheets. From the images of high magnification (inset

of Fig. 4a), the thickness of CRGO is measured at ca. 2.4 nm. It suggests the presence of at least 2–3 layers of reduced GO sheets as the reported thickness for the single-layer reduced GO sheet is ~1 nm (Stankovich et al., 2006). For comparison, HRGO has a thickness of ca. 2.4 nm (inset of Fig. 4b), which is identical to the CRGO thickness. The presence of few layers of reduced GO sheets is attributed to the restacking of layers in the absence of stabilizing molecules.

ATR-FTIR spectra of GO, CRGO and HRGO are shown in Fig. 5. The presence of a broad band at 3287 cm^{-1} (for O-H stretching vibrations), intense narrow bands at 1695 and 1747 cm^{-1} (for C═O stretching vibrations), 1637 cm^{-1} (for O–H bending vibrations), 1233 and 1065 cm^{-1} (for C–O breathing vibrations), and 981 cm^{-1} (for vibrations from epoxy, ether or peroxide groups) indicates the presence of various oxygen functional groups in GO structure (Fig. 5a) (Fernández-Merino et al., 2010). After β-carotene reduction, the intensity of the bands associated to oxygen functional groups decreases to a great extent, indicating the removal of oxygen functional groups on CRGO (Fig. 5b). In addition, some of the bands are slightly shifted due to the change of hydrophobic chemical environment (contains merely carbon–carbon bonds) in the deoxygenated sample compared to the initial GO. The pattern of IR spectrum of CRGO, interestingly, is almost similar to the one of HRGO (Fig. 5c).

The organic moiety and thermal stability of GO, CRGO and HRGO were studied with TGA analysis. The mass loss at a temperature below 100 °C due to the removal of absorbed water can be seen for all samples (Fig. 6). For GO, two stages of mass loss are shown; the first stage starts at 150 °C is due to the loss of hydroxyl, epoxy functional groups and remaining water molecules (Fig. 6a). The second stage (450–650 °C) involves the pyrolysis of the remaining oxygen-containing groups as well as the burning of ring carbon (Jeong et al., 2009). At a temperature of 700 °C, GO shows a total mass loss of 71.3% while CRGO and HRGO only experience mass losses of 21.6% and 16.4%, respectively (Figs. 6b and c). The findings suggest that most of the labile oxygen functional groups have been removed from CRGO and HRGO after reduction process.

Raman spectroscopy is a powerful non-destructive tool to characterize electronic structure of carbonaceous materials. The Raman spectra of GO and CRGO are shown in Fig. 7a and b. There are two main features in Raman spectra for GO and reduced GO, namely G band (ca. 1580 cm^{-1}) and D band (ca. 1345 cm^{-1}). The G band is assigned to the first order scattering of E_{2g} phonon of sp^2 carbon atoms, while the D band is the breathing mode of κ-point phonons of A_{1g} symmetry (Fan et al., 2011). Furthermore, the ratio of peak intensity of D and G bands (I_D/I_G) also provides information on the distance between defects in graphene and it increases with increasing mean distance between two defects (Lucchese et al., 2010; Cancado et al., 2011). The I_D/I_G ratio for GO and CRGO is computed and found to be 0.86 and 1.01, respectively. This could be related to the removal of functional groups and the formation of defects in CRGO (Moon et al., 2010). Furthermore, the I_D/I_G ratio of CRGO is almost identical to that of HRGO (1.08, Fig. 7c). Thus, these data suggest that the reduction process by β-carotene, without any doubt, produces similar results as hydrazine.

3.3. Proposed reduction mechanism of GO by β-carotene

The reduction of GO by β-carotene is promising and hence a mechanism for GO reduction by β-carotene is proposed (Fig. 8). The reaction starts with the addition of oxygen molecule at the central double bond of β-carotene to form epoxide group (Step 1). The epoxide then undergoes hydrolysis resulting in the formation of a diol group (Step 2). Due to the electron donating effect of conjugated double bond in β-carotene, the two protons from the diol group are readily dissociated to form oxygen anions (Woggon, 2002). The oxygen anions act as nucleophiles and attack epoxide moiety of GO through S_N2 pathway. As a result, the oxirane ring is opened up and a water molecule is eliminated to yield aldehydes and CRGO as the final products (Steps 3–5). On the other hand, other oxygen

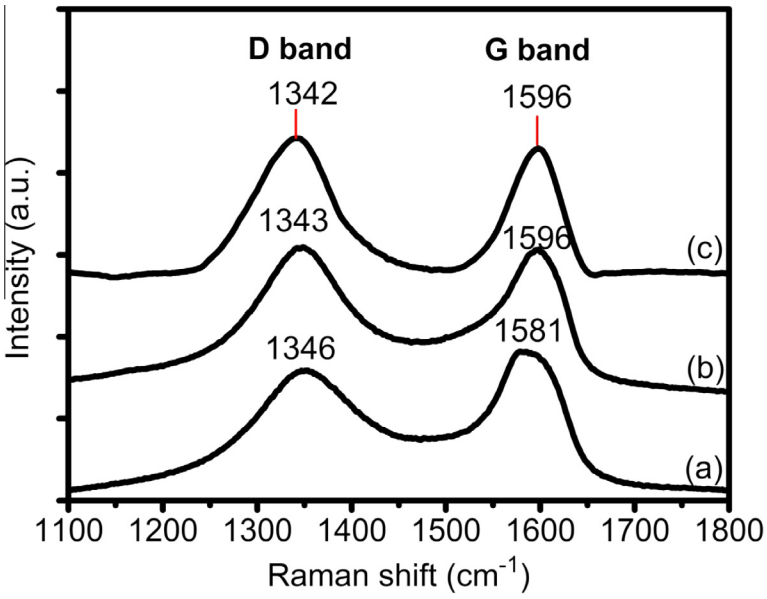

Figure 7 Raman spectra of (a) GO, (b) CRGO and (c) HRGO.

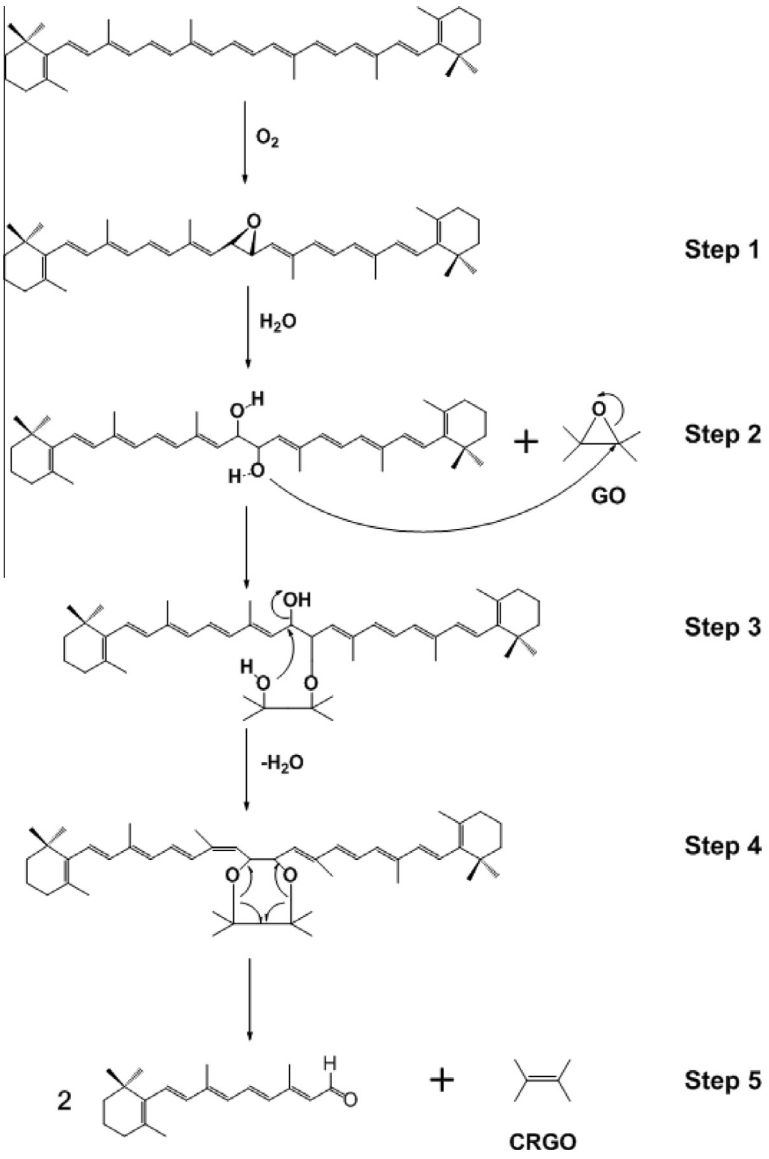

Figure 8 Proposed reduction mechanism of GO to CRGO by β-carotene.

functional groups on GO such as hydroxyl group also experience a similar nucleophilic attack by the oxygen anions to form CRGO as final product.

The reduction mechanism and the formation of aldehydes after CRGO synthesis were verified with FTIR spectroscopy. Fig. 9 shows the FTIR spectra of β-carotene solution before and after reduction reaction. As shown, an additional IR absorption band at 1650 cm^{-1} corresponding to the carbonyl group of aldehyde is detected for the β-carotene solution after reduction. Thus, the observation of IR analysis further supports the findings of spectroscopy, thermogravimetry and proposed mechanism.

3.4. Electrochemical study

The charge storage properties of CRGO were evaluated by cyclic voltammetry (CV) and galvanostatic charge/discharge analyses. In CV study, the specific capacitance is calculated by integrating over the CV curve. As shown in Fig. 10, CRGO exhibits a rectangular shape in CV curve which is an indication of good charge propagation within the structure. The variation of CRGO specific capacitance as a function of scan rate is also measured and is summarized in the inset of Fig. 10. It can be clearly seen that the specific capacitance is dependent on the scan rate whereby the specific capacitance increases at a lower scan rate. The finding is attributed to the diffusion and penetration of ions into CRGO internal sheets at a low scan rate, leading to more ion adsorption that contributes to a higher specific capacitance. From the CV experiment, the maximum specific capacitance attained on CRGO is 142 F/g at 10 mV/s. The maximum specific capacitance of HRGO is also measured, and is just slightly higher (150 F/g at 10 mV/s) than that of CRGO (Fig. 10c). Interestingly, the specific capacitance value of CRGO is much higher than the reported value of RGO produced by other natural reducing agents such as phytoextracts (21 F/g)) (Thakur and Karak, 2012).

The galvanostatic charge/discharge curves for GO, CRGO and HRGO are shown in Fig. 11. The specific capacitance is

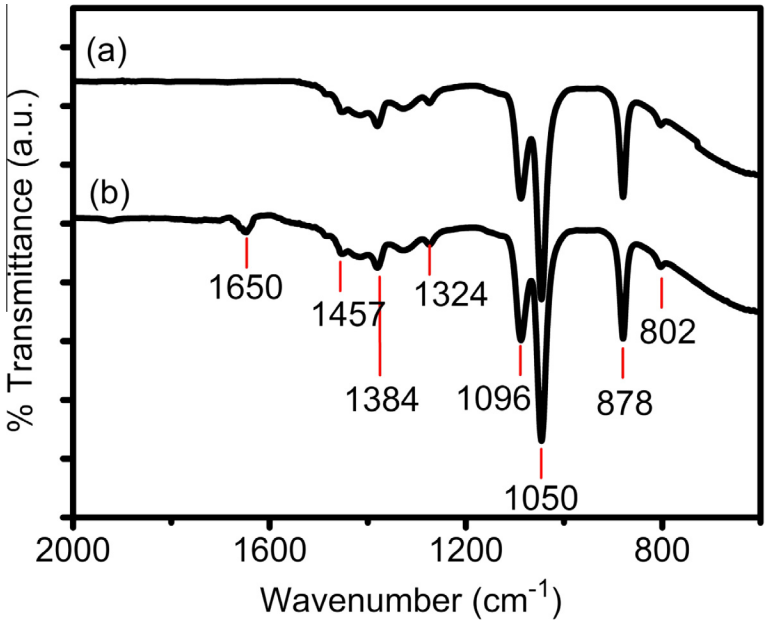

Figure 9 FTIR spectra of β-carotene reaction solution (a) before, and (b) after reduction process.

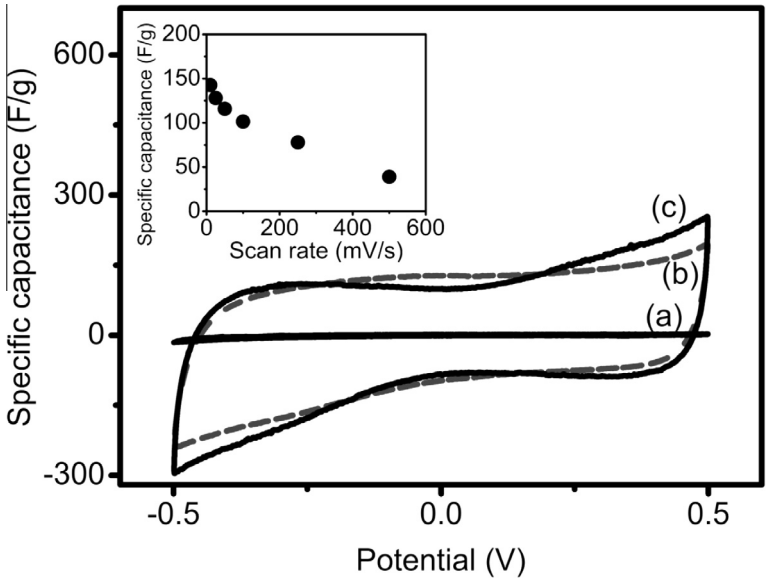

Figure 10 CV curves of (a) GO, (b) CRGO and (c) HRGO in 1.0 M Na_2SO_4 at 100 mV/s. Inset: Variation of specific capacitance as a function of scan rate for CRGO in 1.0 M Na_2SO_4.

calculated from the slope of the discharge curve. It is clearly shown that the charge/discharge curve for CRGO is linear and symmetrical without significant iR drop, indicating the rapid current–voltage response and good charge discharge reversibility of CRGO. Variation of the specific capacitance of CRGO as a function of current density is also obtained and is summarized as the inset of Fig. 11. From charge/discharge experiment, the highest specific capacitance attained on CRGO is 149 F/g at 1 A/g, comparable to 158 F/g obtained on HRGO. Prior to analysis, similar experiments were done on GO electrode. As shown in Figs. 10 and 11a, both the CV and galvanostatic charge/discharge curves indicate that GO contributes negligible amounts of capacitance. Electrode stability represents an important element in the characterization of supercapacitor electrode. Fig. 12 summarizes the CRGO electrode stability, cycled at 1 A/g for 1000 cycles. It is interesting to observe the CRGO electrode possesses high stability with capacitance retention of 89% after 1000 cycles. Furthermore, the charge/discharge curves remain unchanged after 1000 cycles, suggesting the suitability of CRGO as supercapacitor electrode (inset of Fig. 12).

Thus, by comparing with the HRGO which is prepared by using highly toxic and explosive reductant, β-carotene offers us another safe replacement for the reducing agent since it is natural, non-toxic and eco-friendly for deoxygenation reaction. Furthermore, CRGO has good charge storage properties as

Please cite this article in press as: Zaid, R.M. et al., Reduction of graphene oxide nanosheets by natural beta carotene and its potential use as supercapacitor electrode. Arabian Journal of Chemistry (2014), http://dx.doi.org/10.1016/j.arabjc.2014.11.036

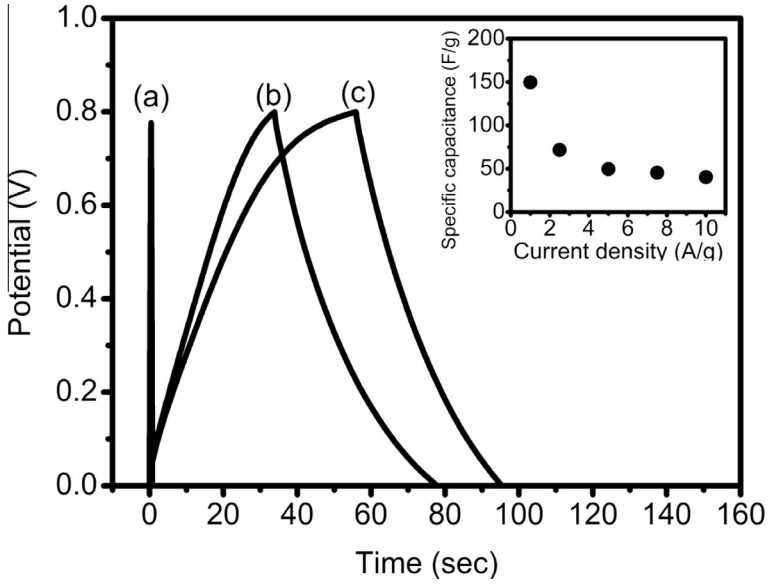

Figure 11 Galvanostatic charge discharge of (a) GO, (b) HRGO, and (c) CRGO in 1.0 M Na_2SO_4 at 2.5 A/g. Inset: Variation of specific capacitance as a function of current density for CRGO in 1.0 M Na_2SO_4.

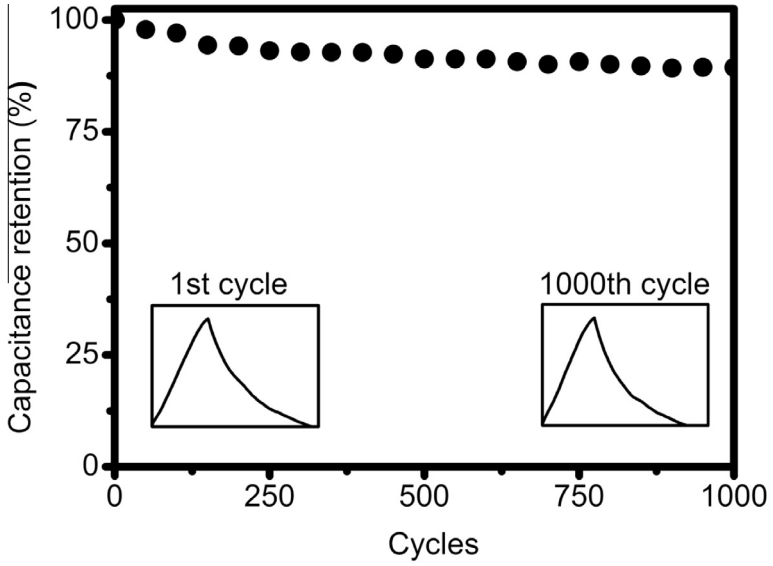

Figure 12 Stability test of CRGO at 1 A/g for 1000 cycles in 1.0 M Na_2SO_4. Insets: Charge discharge curves at 1th cycle and 1000th cycle.

proven by the electrochemical study, and hence, offers another possibility to use environmentally benign β-carotene in the production of graphene as supercapacitor electrode and in nanotechnology applications.

4. Conclusions

In conclusion, the current work reports the potential use of natural, eco-friendly and non-toxic β-carotene as reducing agent for GO reduction. The oxygen scavenging property of β-carotene successfully removes oxygen functionalities on GO nanosheets. The reduction optimization study shows that complete reduction can be achieved within 16 h using 10 mM of β-carotene. Furthermore, spectroscopic and microscopic analyses indicate that the reduction efficacy of β-carotene is comparable to the commonly used hydrazine reducing agent. The electrochemical study also reveals that the CRGO has good charge storage properties, and offers the green replacement possibility of β-carotene in the production of graphene as supercapacitor electrode.

Acknowledgements

K.F. Chong and co-workers would like to acknowledge the funding from the Ministry of Education Malaysia in the form of MTUN-COE (RDU121212 & RDU121213) and ERGS (RDU120406).

References

Balandin, A.A., 2011. Thermal properties of graphene and nanostructured carbon materials. Nat. Mater. 10, 569–581.
Bao, Q., Zhang, H., Wang, B., Ni, Z., Lim, C.H.Y.X., Wang, Y., Tang, D.Y., Loh, K.P., 2011. Broadband graphene polarizer. Nat. Photon. 5, 411–415.
Cancado, L.G., Jorio, A., Ferreira, E.H.M., Stavale, F., Achete, C.A., Capaz, R.B., Moutinho, M.V.O., Lombardo, A., Kulmala, T.S., Ferrari, A.C., 2011. Quantifying defects in graphene via Raman spectroscopy at different excitation energies. Nano Lett. 11, 3190–3196.
Ciccone, M.M., Cortese, F., Gesualdo, M., Carbonara, S., Zito, A., Ricci, G., De Pascalis, F., Scicchitano, P., Riccioni, G., 2013. Dietary intake of carotenoids and their antioxidant and anti-inflammatory effects in cardiovascular care. Mediators Inflamm. 2013, 1–11.
Fan, Z.J., Kai, W., Yan, J., Wei, T., Zhi, L.J., Feng, J., Ren, Y.M., Song, L.P., Wei, F., 2011. Facile synthesis of graphene nanosheets via Fe reduction of exfoliated graphite oxide. ACS Nano 5, 191–198.
Feng, Y., Feng, N., Du, G., 2013. A green reduction of graphene oxide via starch-based materials. RSC Adv. 3, 21466–21474.
Fernández-Merino, M.J., Guardia, L., Paredes, J.I., Villar-Rodil, S., Solís-Fernández, P., Martínez-Alonso, A., Tascón, J.M.D., 2010. Vitamin C is an ideal substitute for hydrazine in the reduction of graphene oxide suspensions. J. Phys. Chem. C 114, 6426–6432.
Gao, J., Liu, F., Liu, Y., Ma, N., Wang, Z., Zhang, X., 2010. Environmental-friendly method to produce graphene that employs vitamin C and amino acid. Chem. Mater. 22, 2213–2218.
Haghighi, B., Tabrizi, M.A., 2013. Green-synthesis of reduced graphene oxide nanosheets using rose water and a survey on their characteristics and applications. RSC Adv. 3, 13365–13371.
Hummers, W., Offeman, R., 1958. Preparation of graphitic oxide. J. Am. Chem. Soc. 80, 1339-1339.
Ismach, A., Druzgalski, C., Penwell, S., Schwartzberg, A., Zheng, M., Javey, A., Bokor, J., Zhang, Y., 2010. Direct chemical vapour deposition of graphene on dielectric surfaces. Nano Lett. 10, 1542–1548.
Jeon, I.Y., Choi, H.J., Choi, M., Seo, S.M., Jung, S.M., Kim, M.J., Zhang, S., Zhang, L., Xia, Z., Dai, L., Park, N., Baek, J.B., 2013. Facile, scalable synthesis of edge-halogenated graphene nanoplatelets as efficient metal-free eletrocatalysts for oxygen reduction reaction. Sci. Rep. 3, 1–7.
Jeong, H.K., Lee, Y.P., Jin, M.H., Kim, E.S., Bae, J.J., Lee, Y.H., 2009. Thermal stability of graphite oxide. Chem. Phys. Lett. 470, 255–258.
Khanra, P., Kuila, T., Kim, N.H., Bae, S.H., Yu, D.S., Lee, J.H., 2012. Simultaneous bio-functionalization and reduction of graphene oxide by baker's yeast. Chem. Eng. J. 183, 526–533.
Kuila, T., Bose, S., Khanra, P., Mishra, A.K., Kim, N.H., Lee, J.H., 2012. A green approach for the reduction of graphene oxide by wild carrot root. Carbon 50, 914–921.
Lee, C., Wei, X., Kysar, J.W., Hone, J., 2008. Measurement of the elastic properties and intrinsic strength of monolayer graphene. Science 321, 385–388.
Li, D., Muller, M.B., Gilje, S., Kaner, R.B., Wallace, G.G., 2008. Processable aqueous dispersions of graphene nanosheets. Nat. Nanotechol. 3, 101–105.
Lucchese, M.M., Stavale, F., Ferreira, E.H.M., Vilani, C., Moutinho, M.V.O., Capaz, R.B., Achete, C.A., Jorio, A., 2010. Quantifying ion-induced defects and Raman relaxation length in graphene. Carbon 48, 1592–1597.
Moon, I.K., Lee, J., Ruoff, R.S., Lee, H., 2010. Reduced graphene oxide by chemical graphitization. Nat. Commun. 1, 73–78.
Mukhopadhyay, A., Guo, F., Tokranov, A., Xiao, X., Hurt, R.H., Sheldon, B.W., 2013. Engineering of graphene layer orientation to attain high rate capability and anisotropic properties in Li-ion battery electrodes. Adv. Funct. Mater. 23, 2397–2404.
Ng, Y.H., Iwase, A., Kudo, A., Amal, R., 2010. Reducing graphene oxide on a visible-light BiVO4 photocatalyst for enhanced photoelectrochemical water splitting. J. Phys. Chem. Lett. 1, 2607–2612.
Novoselov, K.S., Geim, A.K., Morozov, S.V., Jiang, D., Katsnelson, I., Grigorieva, I.V., Dubonos, S.V., Firsov, A.A., 2005. Two-dimensional gas of massless Dirac fermions in graphene. Nature 438, 197–200.
Novoselov, K.S., Geim, A.K., Morozov, S.V., Jiang, D., Zhang, Y., Dubonos, S.V., Grigorieva, I.V., Firsov, A.A., 2004. Electric field effect in atomically thin carbon films. Science 306, 666–669.
Park, S., Ruoff, R.S., 2009. Chemical methods for the production of graphenes. Nat. Nanotechol. 4, 217–224.
Petrone, N., Dean, C.R., Meric, I., Van der Zande, A.M., Huang, P.Y., Wang, L., Muller, D., Shepard, K.L., Hone, J., 2012. Chemical vapor deposition-derived graphene with electrical performance of exfoliated graphene. Nano Lett. 12, 2751–2756.
Pruna, A., Pullini, D., Busquets, D., 2013. Influence of synthesis conditions on properties of green-reduced graphene oxide. J. Nanopart. Res. 15, 1605–1606.
Schedin, F., Geim, A.K., Morozov, S.V., Hill, E.W., Blake, P., Katsnelson, M.I., Novoselov, K.S., 2007. Detection of individual gas molecules adsorbed on graphene. Nat. Mater. 6, 652–655.
Stankovich, S., Dikin, D.A., Dommett, G.H.B., Kohlhaas, K.M., Zimney, E.J., Stach, E.A., Piner, R.D., Nguyen, S.T., Ruoff, R.S., 2006. Graphene-based composite materials. Nature 442, 282–286.
Stankovich, S., Dikin, D.A., Piner, R.D., Kohlhaas, K.A., Kleinhammes, A., Jia, Y., Wu, Y., Nguyen, S.T., Ruoff, R.S., 2007. Synthesis of graphene-based nanosheets via chemical reduction of exfoliated graphite oxide. Carbon 45, 1558–1565.
Stoller, M.D., Park, S., Zhu, Y., An, J., Ruoff, R.S., 2008. Graphene-based ultracapacitors. Nano Lett. 8, 3498–3502.
Strupinski, W., Grodecki, K., Wysmolek, A., Stepniewski, R., Szkopek, T., Gaskell, P.E., Grüneis, A., Haberer, D., Bozek, R., Krupka, J., Baranowski, J.M., 2011. Graphene epitaxy by chemical vapor deposition on SiC. Nano Lett. 11, 1786–1791.
Thakur, S., Karak, N., 2012. Green reduction of graphene oxide by aqueous phytoextracts. Carbon 50, 5331–5339.
Wang, Y., Chen, X., Zhong, Y., Zhu, F., Loh, K.P., 2009. Large area, continuous, few-layered graphene as anodes in organic photovoltaic devices. Appl. Phys. Lett. 95, 063302–063303.
Wang, Y., Shi, Z., Yin, J., 2011. Facile synthesis of soluble graphene via a green reduction of graphene oxide in tea solution and its biocomposites. ACS Appl. Mater. Interfaces 3, 1127–1133.
Woggon, W.D., 2002. Oxidative cleavage of carotenoids catalyzed by enzyme models and beta-carotene 15,15′-monooxygenase. Pure Appl. Chem. 74, 1397–1408.
Xu, L.Q., Yang, W.J., Neoh, K.-G., Kang, E.-T., Fu, G.D., 2010. Dopamine-induced reduction and functionalization of graphene oxide nanosheets. Macromolecules 43, 8336–8339.
Zhang, J., Yang, H., Shen, G., Cheng, P., Zhang, J., Guo, S., 2010. Reduction of graphene oxide via L-ascorbic acid. Chem. Commun. 46, 1112–1114.
Zhu, C., Guo, S., Fang, Y., Dong, S., 2010. Reducing sugar: new functional molecules for the green synthesis of graphene nanosheets. ACS Nano 4, 2429–2437.

Please cite this article in press as: Zaid, R.M. et al., Reduction of graphene oxide nanosheets by natural beta carotene and its potential use as supercapacitor electrode. Arabian Journal of Chemistry (2014), http://dx.doi.org/10.1016/j.arabjc.2014.11.036